

Properties of Building and Plastic Materials in the THz Range

R. Piesiewicz · C. Jansen · S. Wietzke · D. Mittleman ·
M. Koch · T. Kürner

Received: 24 January 2007 / Accepted: 12 March 2007
© Springer Science + Business Media, LLC 2007

Abstract We present measurements of the frequency dependent refractive index and absorption coefficient of a variety of common building and plastic materials between 100 and 1000 GHz. Accurate knowledge of the material parameters is indispensable for the modeling of bound media propagation phenomena including single and multiple reflections, transmission, diffraction and scattering effects. These models are for example required for a reliable channel simulation to investigate signal propagation in future wireless communication systems operating with Gigabit data rates at frequencies above 100 GHz. Also, the measured material parameters can be used for the investigation and development of THz system components.

Keywords Material properties · Millimeterwaves · Submillimeterwaves · Terahertz · THz channel modeling

1 Introduction

In recent years, research on wireless communication systems with carrier frequencies above 100 GHz [1, 2] has been intensified. The incentive for this spectral shift results from the

R. Piesiewicz · T. Kürner
Institut für Nachrichtentechnik, Technische Universität Braunschweig,
Schleinitzstraße 22, 38106 Braunschweig, Germany

C. Jansen · S. Wietzke · M. Koch
Institut für Hochfrequenztechnik, Technische Universität Braunschweig,
Schleinitzstraße 22, 38106 Braunschweig, Germany

D. Mittleman
Electrical and Computer Engineering Department, Rice University,
6100 Main Street, Houston, TX 77005, USA

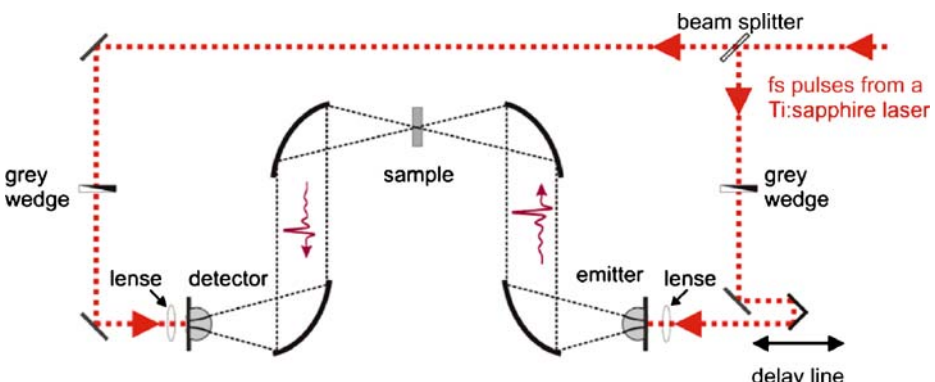
R. Piesiewicz (✉) · S. Wietzke · M. Koch · T. Kürner
Terahertz Communications Lab, Technische Universität Braunschweig,
Schleinitzstraße 22, 38106 Braunschweig, Germany
e-mail: r.piesiewicz@ieee.org

Table 1 List of measured materials.

Material type	Sample number	Sample name	x, y in mm	d, σ in mm
Wood	W1	Laminated beech wood (glued wood)	40, 40	5.08, 0.047
	W2	Lumber-core plywood (fir)	40, 40	5.21, 0.02
	W3	High-Density Fiberboard (HDF)	40, 40	3.56, 0.028
	W4	Chipboard	40, 40	4.99, 0.033
	W5	Medium-Density Fiberboard (MDF)	40, 40	4.91, 0.02
	W6	Fir wood	40, 40	5.32, 0.027
	W7	Laminated pine wood (glued wood)	40, 40	4.92, 0.305
Brick	B1	Sand-lime brick	40, 40	7.17, 0.14
	B2	Clay brick	40, 40	7.18, 0.061
	B3	Gypsum plaster (Rigips without cardboard)	40, 40	8.20, 0.13
Plastic	P1	Polystyrene (PS)	40, 40	1.49, 0.002
	P2	Polycarbonate (PC)	40, 40	3.65, 0.0
	P3	Glass fiber-reinforced laminate	60, 60	2.81, 0.004
	P4	Polyvinyl chloride (PVC)	60, 60	6.13, 0.028
	P5	High-Density Polyethylene (HDPE)	65, 65	6.17, 0.0
	P6	Clear cast acrylic (plexiglass)	60, 60	5.26, 0.099
	P7	Polyamide 6 (PA 6)	60, 60	2.09, 0.01
	P8	Polyamide 66 (PA 66)	60, 60	2.08, 0.006
Glass	G1	Glass (typical window pane)	40, 40	2.92, 0.0

estimated data rates required by future wireless applications [3]. As tens of Gbits will be needed, a high bandwidth is mandatory which could be provided by systems with center frequencies between 100 and 1000 GHz in atmospheric windows where the gaseous attenuation is relatively low. Especially, the frequencies above 300 GHz are of interest, as they are still unregulated [4].

Before such systems can be introduced, the indoor radio channel must be thoroughly characterized in order to gain understanding of propagation phenomena, establish link budgets and analyze potential application scenarios. For this purpose, direct channel measurements can be supported by simulation tools. For example, site-specific ray-tracing can be employed efficiently to calculate the spatial and temporal channel properties for given scenarios [5]. In order to obtain accurate channel predictions, the ray-tracing needs

**Fig. 1** Conventional THz TDS system used for the measurements of plastic samples.

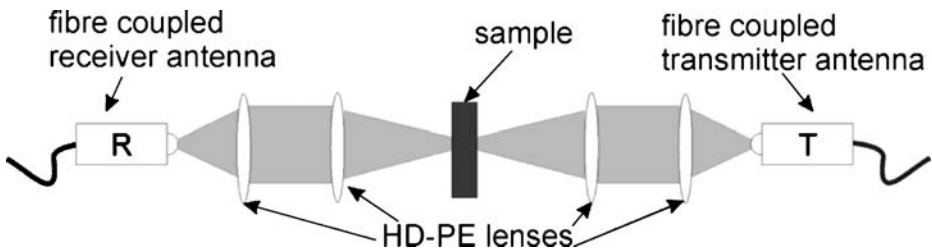


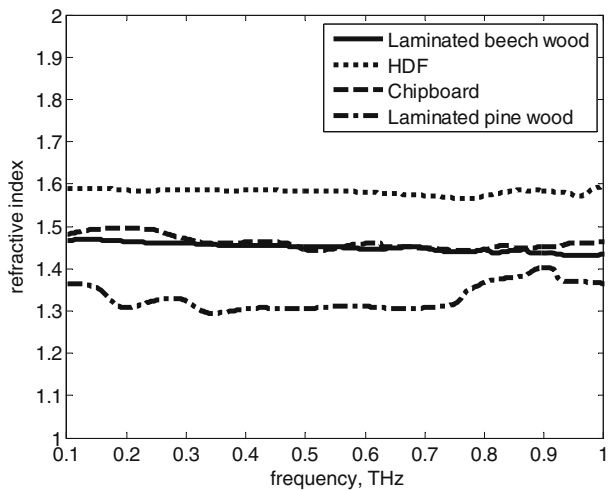
Fig. 2 Fibre coupled THz TDS system used for the measurements of glass, wood and brick samples.

reliable analytical models of bound-media propagation phenomena. In particular, schemes for the calculation of reflection and transmission [6, 7], diffraction [8, 9] and scattering [10, 11] effects are required. Common to these models is their dependence on the material parameters, i.e. refractive index and absorption coefficient. Hence, only the exact knowledge of these parameters in a wide frequency range allows for reliable simulations of signal propagation in future broadband wireless communication systems. Although a wealth of measurements of electrical properties of different materials above 100 GHz is reported [12, 13], corresponding data for building materials, which is required for the propagation prediction in indoor environments, is very rare in the literature [6, 14]. In this paper, we report the measurements of material properties for a wide choice of different building materials (wood, brick, plastic) in the frequency range between 100 and 1000 GHz. Additionally we show the measurements of a variety of common plastic materials, which might be useful for the investigation and development of THz system components.

Table 2 Measurement results of the samples.

Sample	n , σ_n	$\alpha_{100 \text{ GHz}}, \sigma$ in cm^{-1}	$\alpha_{350 \text{ GHz}}, \sigma$ in cm^{-1}	$\alpha_{500 \text{ GHz}}, \sigma$ in cm^{-1}	$\alpha_{700 \text{ GHz}}, \sigma$ in cm^{-1}
W1	1.45, 0.014	1.79, 0.13	6.3, 0.09	9.98, 0.39	-
W2	1.40, 0.077	1.85, 0.43	6.45, 1.62	9.80, 2.99	-
W3	1.58, 0.031	1.85, 0.15	7.87, 1.20	13.6, 1.67	-
W4	1.46, 0.014	2.86, 0.37	11.4, 1.88	16.9, 1.47	-
W5	1.46, 0.007	1.16, 0.09	4.61, 0.25	7.79, 0.45	13.1, 2.59
W6	1.33, 0.070	1.74, 0.54	5.86, 2.40	8.20, 3.08	11.9, 3.14
W7	1.33, 0.001	1.67, 0.02	8.14, 0.20	10.1, 0.01	-
B1	1.87, 0.016	1.71, 0.21	9.09, 1.05	-	-
B2	1.87, 0.008	0.86, 0.05	4.82, 0.02	9.16, 0.21	-
B3	1.60, 0.028	0.51, 0.06	6.22, 0.83	-	-
P1	1.59, 0.001	0.28, 0.35	0.49, 0.32	1.00, 0.12	1.75, 0.39
P2	1.66, 0.000	0.44, 0.05	1.96, 0.04	3.67, 0.05	11.1, 0.28
P3	2.14, 0.010	1.32, 0.11	7.15, 0.69	13.9, 0.88	35.5, 6.36
P4	1.67, 0.003	0.39, 0.05	3.33, 0.14	6.44, 0.21	11.5, 1.61
P5	1.53, 0.000	0.06, 0.14	0.11, 0.08	0.22, 0.08	0.38, 0.11
P6	1.61, 0.001	0.59, 0.21	2.62, 0.29	4.93, 0.26	14.5, 1.21
P7	1.74, 0.005	1.36, 0.98	3.85, 0.82	7.35, 0.93	24, 2.78
P8	1.74, 0.007	0.90, 0.48	3.03, 0.28	6.06, 0.53	21.8, 2.34
G1	2.58, 0.001	1.95, 0.08	9.95, 0.14	17.2, 0.14	-

Fig. 3 Refractive indices of wood samples: laminated beech wood, HDF, chipboard, laminated pine wood.



2 Measurements

The investigated samples comprise three groups: wood materials, plastic materials and brick materials. Additionally, glass as found in typical window panes is examined.

Measured materials are listed in Table 1. The lateral dimensions of the samples x, y and their thickness are also specified. For each of the samples the thickness is measured at five different positions and the mean values d together with their corresponding standard deviations are given.

We measure the absorption coefficient and the refractive index of the samples with THz time-domain spectroscopy (THz TDS) in transmission geometry. The measurements are performed with two different THz TDS transmission setups as illustrated in Figs. 1 and 2. The first setup (Fig. 1) is a conventional free-space THz spectrometer [15], while the second one (Fig. 2) uses fibres to direct the optical femtosecond pulses on the photoconducting

Fig. 4 Refractive indices of wood samples: lumber-core plywood (fir), MDF, fir wood.

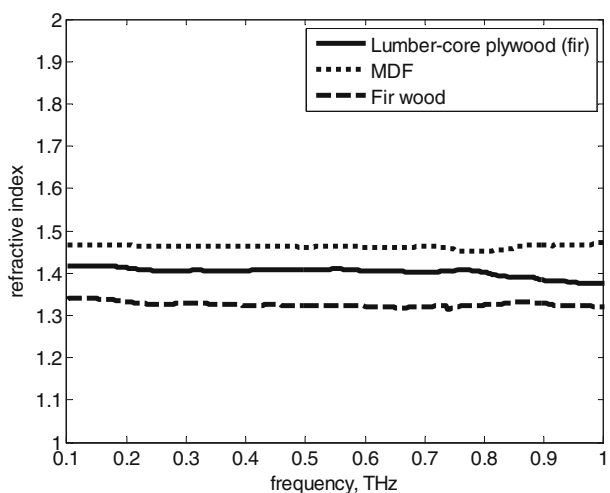
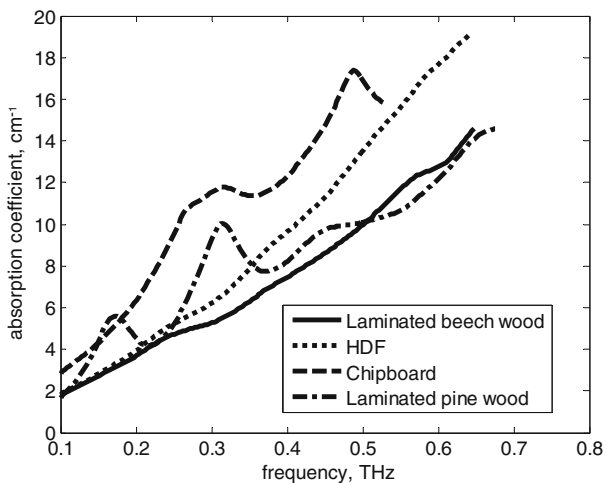


Fig. 5 Absorption coefficients of wood samples: laminated beech wood, HDF, chipboard, laminated pine wood.



antennas (Picometrix T-Ray 2000™) [16]. The conventional setup is employed for the measurements of the plastic samples, while the glass, wood and brick samples are measured with the fibre coupled one. The frequency dependent focal spot size of the Gaussian shaped THz beam is in the range of few millimetres and is considerably smaller than the lateral dimensions of the samples. The peak dynamic range of the conventional system is near 58 dB. Without a sample in the propagation path, the system bandwidth is 2.0 THz. In case of the measurement system from Fig. 2, the available bandwidth is 1.1 THz and the peak dynamic range amounts to around 48 dB. The impulse duration of the femtosecond Ti: Al₂O₃ laser is 20 fs for the conventional system and 80 fs for the coupled fibre one.

In the experiments, a sample pulse with and a reference pulse without the sample in the propagation path are measured. A window function is applied to the time-domain data to remove unwanted multiple reflections. The frequency dependent indices of refraction $n(f)$ and absorption coefficients $\alpha(f)$ of the samples are calculated from the phase and amplitude information of the Fourier spectra of the pulses in the frequency range between 0.1 and

Fig. 6 Absorption coefficients of wood samples: lumber-core plywood, MDF, fir wood.

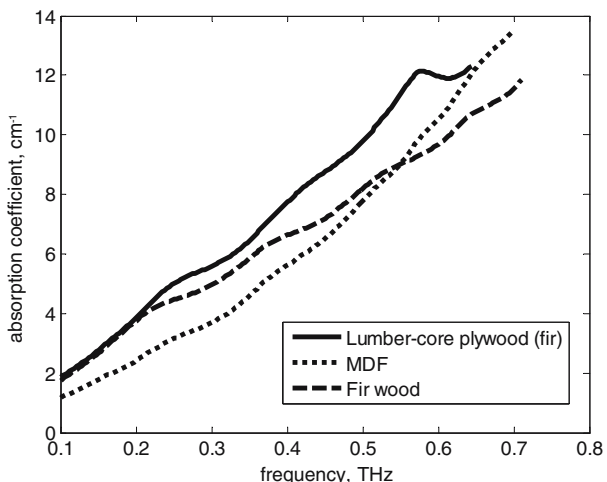
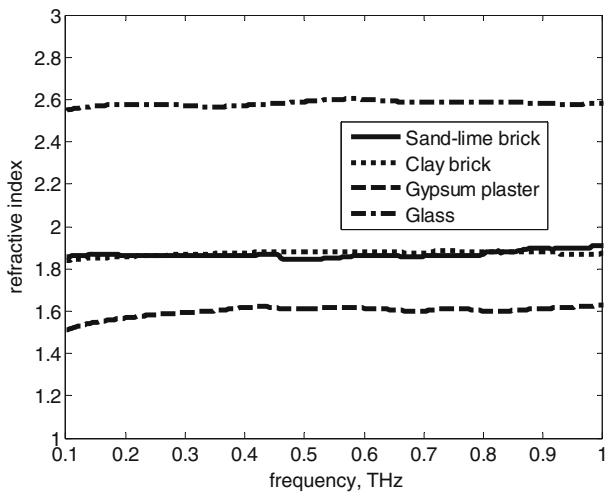


Fig. 7 Refractive indices of brick samples and glass: sand-lime brick, clay brick, gypsum plaster, window glass.



1.0 THz [17]. These measurements are performed on samples with smooth surfaces to avoid scattering.

To assure high accuracy of the results, each of the samples is measured at five different positions. Statistical analysis is then performed on the acquired data sets. This is especially important for the building materials, as these samples are not chemically pure. Hence, a slight spatial variation in the material parameters is possible, which then results in a higher standard deviation. In Table 2 the measured material parameters are listed.

Refractive indices do not vary considerably with frequency. Hence, they are tabulated as average values for respective sets of measurements, whereas for each measurement they are first spectrally averaged in the frequency range between 100 GHz and 1 THz. Here, the corresponding standard deviations are also reported.

All samples exhibit a significant increase of the absorption coefficient with the frequency. Only in case of the PS and HDPE the increase is very slight. The frequency range in which a meaningful absorption coefficient can be calculated is limited by the

Fig. 8 Absorption coefficients of brick samples and glass: sand-lime brick, clay brick, gypsum plaster, window glass.

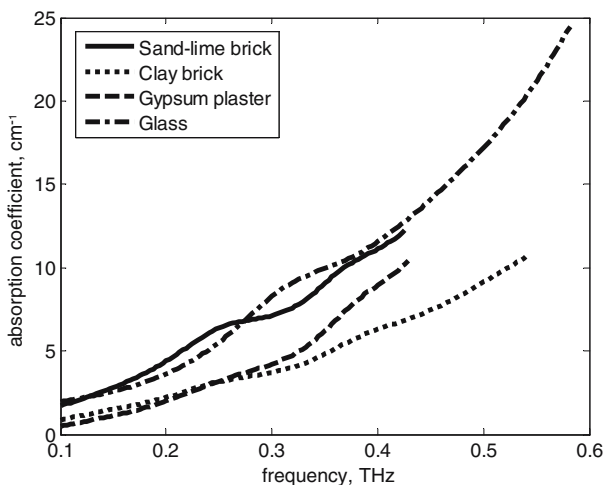
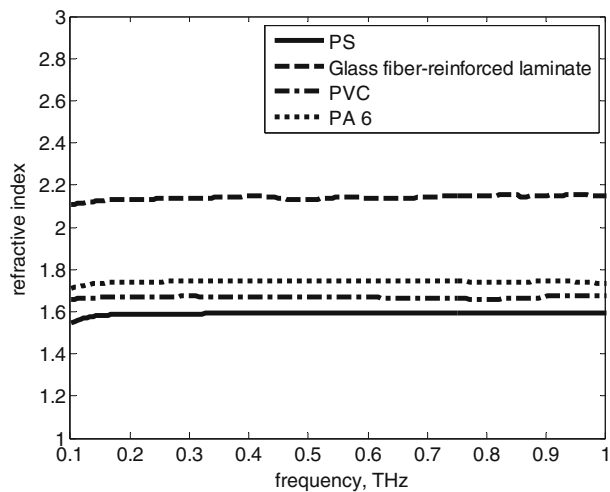


Fig. 9 Refractive indices of plastic samples: polystyrene (PS), glass fiber-reinforced laminate, polyvinyl chloride (PVC), polyamide 6 (PA 6).



dynamic range. The dynamic range is defined by the noise floor and the frequency dependent signal strength of the THz TDS system as well as the thickness and the frequency dependent level of absorption of the sample [18]. While [18] employs the mean value of the spectrum acquired with a completely blocked THz beam for noise floor calculation, we use a more conservative approach by adding twice the standard deviation to the mean value. According to statistical analysis for normally distributed variables, the probability that the noise samples do not surpass their mean value by more than two standard deviations amounts then to 97.72% which is significantly higher than the 50% resulting from the simple mean value calculation [19].

The tabulated values of the absorption coefficients are shown for four different frequencies as averages for respective sets of measurements together with their corresponding standard deviations. The frequencies shown in Table 2 are 100 GHz, which is the lower limit of the frequency range, 350 GHz, which is an atmospheric frequency

Fig. 10 Refractive indices of plastic samples: polycarbonate (PC), high-density polyethylene (HDPE), clear cast acrylic (Plexiglass), polyamide 66 (PA 66).

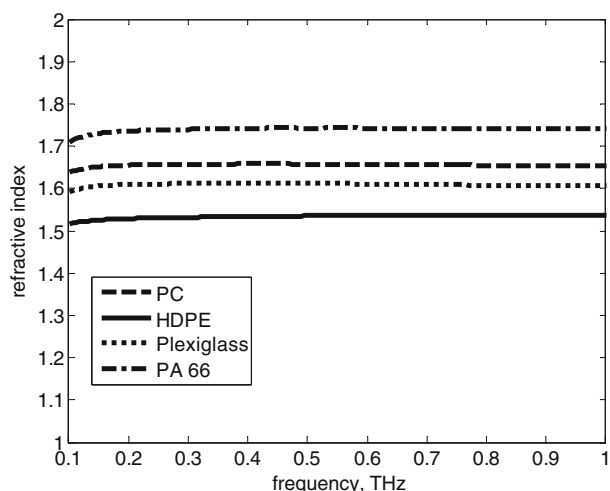
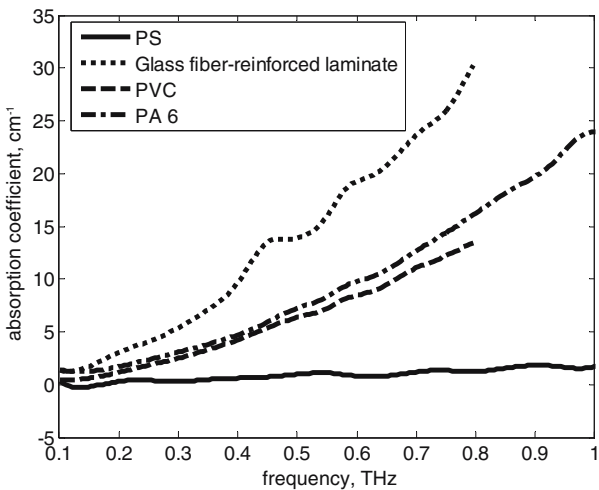


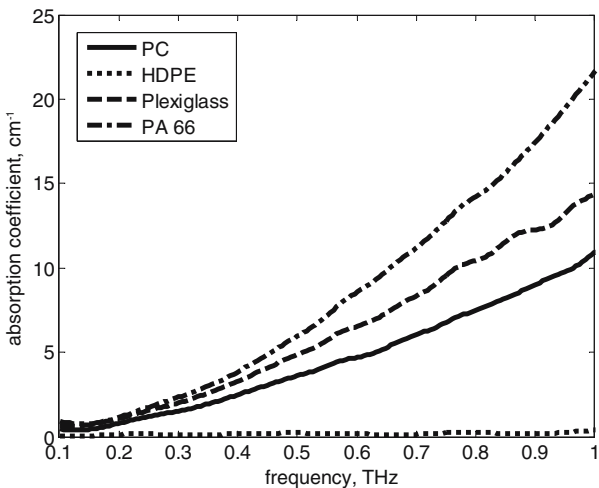
Fig. 11 Absorption coefficients of plastic samples: polystyrene (PS), glass fiber-reinforced laminate, polyvinyl chloride (PVC), polyamide 6 (PA 6).



window, 500 GHz and 700 GHz. For 500 and 700 GHz the limits explained above applied to some samples, so that the corresponding fields are left blank.

In addition to the tabulated transmission data, the refractive indices and absorption coefficients of the samples, averaged for five measurements at a time, are plotted as functions of frequency. The refractive indices are shown for the frequencies between 100 and 1000 GHz, whereas the frequency range of the absorption coefficients is limited individually for each sample as explained above. Figures 3 and 4 show the refractive indices of the investigated wood materials, whereas Figs. 5 and 6 depict the corresponding absorption curves. The refractive indices and absorption coefficients of brick materials and glass are depicted in Figs. 7 and 8, respectively. In Figs. 9 and 10 the refractive indices of plastic materials are plotted, while Figs. 11 and 12 contain the corresponding absorption coefficients.

Fig. 12 Absorption coefficients of plastic samples: polycarbonate (PC), high-density polyethylene (HDPE), clear cast acrylic (Plexiglass), polyamide 66 (PA 66).



3 Conclusions

We show transmission THz TDS measurements of the material parameters of a variety of common building and plastic materials between 100 and 1000 GHz. The measured data can be used for simulations of signal propagation in future ultra-broadband indoor wireless communication systems that will operate at frequencies above 100 GHz. Also, the measured material parameters might be used for the investigation and development of THz system components.

Acknowledgement The authors thank Dr. Martin Bastian and Dr. Karsten Kretschmer from Süddeutsches Kunststoff-Zentrum, Würzburg, Germany, for providing the samples P7 and P8.

References

1. T. Nagatsuma, Exploring sub-terahertz waves for future wireless communications, IEEE 31th Intl. Conf. on IRMMW and 14th Intl. Conf. on Terahertz Electronics, China, September 2006, p. 4.
2. A. Hirata, T. Kosugi, H. Takahashi, R. Yamaguchi, F. Nakajima, T. Furuta, H. Ito, H. Sugahara, Y. Sato, and T. Nagatsuma, 120-GHz-band millimeter-wave photonic wireless link for 10-Gb/s data transmission, *IEEE Trans. Microwave Theor. Tech.* **54**(5), 1937–1944 (2006).
3. S. Cherry, Edholm's law of bandwidth, *IEEE Spectr.* **41**, 19–50 (2004).
4. R. Piesiewicz, T. Kleine-Ostmann, N. Krumbholz, D. Mittleman, M. Koch, and T. Kürner, Concept and perspectives of future ultra broadband THz communication systems, IEEE 31th Intl. Conf. on IRMMW and 14th Intl. Conf. on Terahertz Electronics, China, September 2006, p. 96.
5. R. Piesiewicz, J. Jemai, M. Koch, and T. Kürner, THz channel characterization for future wireless gigabit indoor communication systems, SPIE Intl. Symp. on Integrated Optoelectronic Devices, Terahertz and Gigahertz Electronics and Photonics IV, Vol. 5727, San Jose, USA, January 2005, pp. 166–176.
6. R. Piesiewicz, T. Kleine-Ostmann, N. Krumbholz, D. Mittleman, M. Koch, and T. Kürner, Terahertz characterisation of building materials, *IEE Electron. Lett.* **41**(18), 1002–1004 (2005).
7. M. Born and E. Wolf, *Principles of Optics*. (Pergamon Press, 1964), pp. 36–47.
8. D. A. McNamara, C. W. I. Pistorius, and J. A. G. Malherbe, *Introduction to the Uniform Geometrical Theory of Diffraction*. (Artech House, 1990).
9. A. G. Dimitriou and G. D. Sergiadis, Architectural features and urban propagation, *IEEE Trans. Antennas Propag.* **54**(3), 774–784 (2006).
10. K.F. Warnick and W. C. Chew, Numerical simulation methods for rough surface scattering, *IoP Waves in Random Media* **11**(1), R1–R30 (2001).
11. P. Beckmann and A. Spizzichino, *The Scattering of Electromagnetic Waves from Rough Surfaces* (Artech House, 1987), pp. 80–98.
12. J. W. Lamb, Miscellaneous data on materials for millimetre and submillimetre optics, *Int. J. IR Millim. Waves* **17**(12), 1997–2034 (1996).
13. G. J. Simonis, Index to the literature dealing with the near millimeter-wave properties of materials, *Int. J. IR Millim. Waves* **3**(4), 439–469 (1982).
14. N. Hiromoto, R. Fukasawa, and I. Hosako, Measurement of optical properties of construction materials in the terahertz region, IEEE 31th Intl. Conf. on IRMMW and 14th Intl. Conf. on Terahertz Electronics, China, September 2006, p. 157.
15. M. Hangyo, M. Tani, and T. Nagashima, Terahertz time-domain spectroscopy of solids: a review, *Int. J. IR Millim. Waves* **26**(12), 1661–1690 (2005).
16. D. Mittleman, Terahertz Imaging, in *Sensing with Terahertz Radiation*, edited by D. Mittleman (Springer, 2003), pp. 117–153.
17. L. Duvallet, F. Garet, and J.-L. Coutaz, A reliable method for extraction of material parameters in Terahertz time-domain spectroscopy, *IEEE J. Quantum Electron.* **2**(3), 739–746 (1996).
18. P. U. Jepsen and B. M. Fischer, Dynamic range in terahertz time-domain transmission and reflection spectroscopy, *Optics Lett.* **30**(1), 29–31 (2005).
19. R. S. Burington and D. Curtis, *Handbook of Probability and Statistics with Tables* (McGraw-Hill Book Company, 1970), p. 111.